2009 American Control Conference
Hyatt Regency Riverfront, St. Louis, MO, USA
June 10-12, 2009

Modified ILMI algorithm for practical PID/PD implementation on a Micro Air Vehicle

Neha Satak[§] and M Seetharama Bhat[†]

***Abstract*— This paper extends the iterative linear matrix inequality algorithm (ILMI) for systems having non-ideal PI, PD and PID implementations. The new algorithm uses the practical implementation of the feedback blocks to form the equivalent static output feedback plant. The LMI based synthesis techniques are used in the algorithm to design a multi-loop, multi-objective fixed structure control. The benefits of such a control design technique are brought out by applying it to the lateral stabilizing and tracking feedback control problem of a 30cm wingspan micro air vehicle.**

I. Introduction

Automatic PID tuning algorithms have been extensively worked upon. Algorithms based on modern control techniques like genetic algorithm, fuzzy logic [1] and multi-objective robust tuning [2] are widely used. A brief summary of all these is given by Cominos & Munro [3]. Algorithms based on genetic algorithm and fuzzy logics, search in a wide space and are heuristic. Multi-objective robust tuning methods based on LMI, on the other hand, are less heuristic and use the convex nature of the problem to arrive at the solution. Most of the control design techniques like H_2/H_∞ stability and performance criteria, pole placement and μ-synthesis have equivalent LMI formulations. The simultaneous use of these makes multi-disciplinary control design possible.

To aid the control designers, the LMI based techniques have efficient tools under MATLAB®. Its capabilities are used to design automated algorithms for fixed order multi-objective control designs by ([2], [4], [5]). Linear matrix inequality formulations for analysis of closed loop stability, pole placement in specific region [6] and, H_2/H_∞ robust performance and stability are well developed. For static output feedback systems, many of these formulations for analysis are also used for synthesis. The PID control formulations are therefore converted to equivalent static output feedback(SOF) forms. This conversion is done to take advantage of the multiple loop tuning capability of LMI for SOF systems. The LMI formulations for robust control design and pole placement are used to tune the SOF gains in this paper.

For systems with ideal proportional, differentiated and integrated outputs available for feedback, the SOF formulation can be done as shown by Zheng et al. [4]. Systems like the flight control system on a micro air vehicle are time critical and have low computational power. They use first order practical implementations of integrator and differentiators. In theory, the PID feedback of pitch rate can give a short period damping of 1 for the micro air vehicle when ideal PID implementation is considered. But in practise, this damping reduces due to the extra dynamics introduced by non-ideal integrator and differentiator algorithms used for feedback on the real system. Design using ideal PID implementation is misleading. To obtain more accurate results, the SOF formulation is done while taking into account the computationally less expensive non-ideal PID feedback control structures . The unique mapping of SOF gains to the PID gain domain is guaranteed for the practical integrator and differentiator implementations used.

Modifications are made to the iterative linear matrix algorithm proposed by Bervani & Hiyama [5] for obtaining the SOF gains. Additional constraints, based on gain margin and phase margin, are put to avoid premature termination of the algorithm. The paper proposes the SOF formulation for systems using practical PID implementations in the first section. The next section discusses the modification of previous algorithm. After this the lateral control design for micro air vehicle, Sapthami-flyer, is presented. Simulation results for loiter mode of micro air vehicle is given next, followed by the conclusion.

II. Control Formulation

The original system is converted to its equivalent static output feedback representation. In order to meet the conflicting performance and stability requirements, frequency weighted cost function are augmented to the plant dynamics to obtain the generalized plant.

A. SOF formulation for practical PID implementation

The SOF formulation for the feedback structure in Fig. 1 is sought. Consider that the LTI system G(s) has the following state space representation:

$$\dot{x} = Ax + Bu; \qquad y = Cx + Du; \qquad u = u_1 + r \tag{1}$$

Here, r is the reference input and u is the control input to plant G(s). The output is y and differentiated and integrated outputs are $\mathbf{y_i}$ and $\mathbf{y_d}$ respectively. The ideal differentiator is a non-causal system and hence cannot be ideally implemented. Due to computational limitation, in practice, integrator and differentiator are usually implemented by adding a non-zero pole and zero respectively, far away to minimize their effects. The commonly used non-ideal continuous time

[§] Research Student at Aerospace Engineering, Indian Institute of Science, Bangalore. satku@aero.iisc.ernet.in
[†] Faculty at the Aerospace Engineering, Indian Institute of Science, Bangalore. msbdcl@aero.iisc.ernet.in

978-1-4244-4524-0/09/$25.00 ©2009 AACC

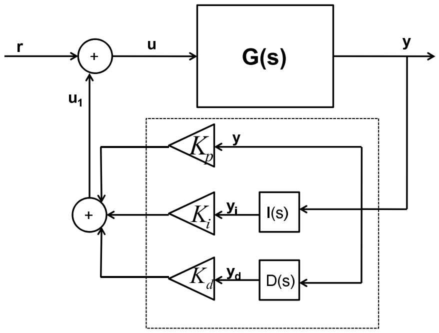

Fig. 1. The Feedback System

implementations of them in the s-domain are I(s) and D(s).

$$I(s) = \frac{c_1 s + c_0}{s} \quad (2)$$

$$D(s) = \frac{c_3 s + c_2}{s + a_1} \quad (3)$$

The feedback u_1 to the plant is given below:

$$u_1 = K_p \mathbf{y(t)} \;+\; K_i \mathbf{y_i(t)} \;+\; K_d \mathbf{y_d(t)}$$

Transfer function for the PID feedback block can be represented by a second order transfer function H(s). Its first companion state space representation is used for the SOF formulation and is given in (4) and (5).

$$H(s) = \frac{U_1(s)}{Y(s)} = K_p + K_i I(s) + K_d D(s) = \frac{b_2 s^2 + b_1 s + b_0}{s(s+a_1)}$$

$$\dot{\mathbf{x_c}} = A_c \mathbf{x_c} + B_c \mathbf{u_c}; \qquad \mathbf{y_c} = C_c \mathbf{x_c} + D_c \mathbf{u_c}$$

$$\dot{\mathbf{x_c}} = \begin{bmatrix} -a_1 & 0 \\ 1 & 0 \end{bmatrix} \mathbf{x_c} + \begin{bmatrix} 1 \\ 0 \end{bmatrix} u_c \quad (4)$$

$$\mathbf{y_c} = \begin{bmatrix} b_1 - a_1 b_2 & b_0 \end{bmatrix} \mathbf{x_c} + b_2 \mathbf{u_c} \quad (5)$$

The system states in (1) are augmented with the $\mathbf{x_c}$ states of the controller to get the augmented states $\tilde{\mathbf{x}}$ of the closed loop system, i.e.,

$$\tilde{\mathbf{x}} = \begin{bmatrix} \mathbf{x} & \mathbf{x_c} \end{bmatrix}'; \qquad \dot{\tilde{\mathbf{x}}} = \overline{A}\tilde{\mathbf{x}} + \tilde{B} r$$

$$\begin{bmatrix} \dot{\mathbf{x}} \\ \dot{\mathbf{x_c}} \end{bmatrix} = \begin{bmatrix} A + BD_cC & BC_c \\ B_cC & A_c \end{bmatrix} \begin{bmatrix} \mathbf{x} \\ \mathbf{x_c} \end{bmatrix} + \begin{bmatrix} B \\ 0 \end{bmatrix} r \quad (6)$$

The equivalent SOF representation of the system is found by decomposing the closed loop system as shown in (7). The decomposition is performed such that the SOF gain $\tilde{\mathbf{K}}$ is a function of the closed loop PID gain matrix K of the fixed PID control structure. $\tilde{A}$, $\tilde{B}$ and $\tilde{C}$ define the open loop SOF system and are therefore required to be not a function of K.

$$\overline{A} = \tilde{A} + \tilde{B}\tilde{\mathbf{K}}\tilde{C} \quad (7)$$

The decomposed matrix is given below:

$$\tilde{A} = \begin{bmatrix} A & 0 \\ \begin{bmatrix} B_cC \\ 0 \end{bmatrix} & A_c \end{bmatrix}; \qquad \tilde{B} = \begin{bmatrix} B \\ 0 \end{bmatrix}; \qquad \tilde{C} = \begin{bmatrix} C & 0 \\ 0 & I \end{bmatrix} \quad (8)$$

The PID gain matrix can be obtained from the SOF gain matrix $\tilde{\mathbf{K}}$ by invertible matrix M from relation (9). Here, $K = [K_p \quad K_i \quad K_d]'$. The invertibility of M is proved next.

$$\tilde{\mathbf{K}} = M\,K \quad (9)$$

Proposition 1: For the above SOF representation M is always invertible.

Proof: An expression for the matrix M is obtained by substituting (4), (5) and (8) in (7). Substituting $\tilde{K} = [K_1\ K_2\ K_3]$ gives us the following expression for M:

$$M = \begin{bmatrix} 1 & c_1 & c_3 \\ 0 & c_0 & c_2 - a_1 c_3 \\ 0 & a_1 c_0 & 0 \end{bmatrix} \quad (10)$$

$$det(M) = a_1 c_0 (c_2 - a_1 c_3) \quad (11)$$

We prove that M is invertible by contradiction. Suppose det(M) is 0. This implies, one of the following cases is true:

1) $a_1 = 0$: if $a_1 = 0$ then the transfer function of differentiator in (3) will have a dominant pole at the origin. Bode magnitude plot for the transfer function will show a fall, instead of rise when the zero is not at the origin. When it is at the origin then it will balance the pole, hence making it a proportional gain system instead of a differentiator. Therefore, a_1 is not equal to 0.

2) $\mathbf{c_0 = 0}$: if c_0 is equal to 0 then the integrator transfer function (2) will reduce to a constant gain c_1. Therefore, this is not possible.

3) $\mathbf{c_2 = a_1 c_3}$: if this is true then the differentiator transfer function have its zero and pole at the same location. These cancel each others effect and it reduces to a gain c_3. This is again not possible.

As none of the above three cases can be true, therefore det(M) is not equal to zero and M is always invertible. Similarly, systems with multiple feedback loops will have M as a block diagonal matrix with each block invertible.

B. Generalized Plant for H_2/H_∞ Control Design

The SOF plant dynamics is augmented by frequency weighted cost functions to obtain the generalized plant $G_i(s)$. The new states of the SOF generalized plant function are $\bar{\mathbf{x}}$. Here, $\mathbf{w}$ is the input disturbance vector and, $\mathbf{z_2}$ and $\mathbf{z_\infty}$ are robust H_2 and H_∞ performance output vectors respectively. The state space representation of $G_i(s)$ is given below.

$$\dot{\bar{\mathbf{x}}} = A_i \bar{\mathbf{x}} + B_y \mathbf{u_1} + B_r r + B_w \mathbf{w} \quad (12)$$

$$\mathbf{z_\infty} = C_\infty \bar{\mathbf{x}} + D_{\infty_w} \mathbf{w} + D_{\infty_{u_1}} \mathbf{u_1} \quad (13)$$

$$\mathbf{z_2} = C_2 \bar{\mathbf{x}} + D_{2_w} \mathbf{w} + D_{2_{u_1}} \mathbf{u_1} \quad (14)$$

$$\mathbf{y} = C_y \bar{\mathbf{x}} + D_y \mathbf{u_1} \quad (15)$$

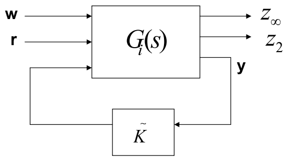

Fig. 2. The Generalized SOF closed loop system

III. The Algorithm

The static output feedback representation for PID feedback is extended to practical integrator and differentiator implementations (see the previous section) for use in ILMI algorithm. It is also proved in the previous section that PID gains can be uniquely obtained from the SOF gains. We now consider the lemma 1 which is used to construct the algorithm.

Lemma 1 [5]: The generalized plant, after feedback, has a H_2 performance index γ and all its poles are at the left hand side of $\sigma = \alpha/2$ in the complex plane, if there exist a SOF gain matrix $\tilde{\mathbf{K}}$ and P such that,

$$\begin{bmatrix} A_iP + PA_i' + B_wB_w' + \Sigma & B_y\tilde{K} + PC_y' \\ (B_y\tilde{K} + PC_y')' & -I \end{bmatrix} < \begin{bmatrix} \alpha P & 0 \\ 0 & 0 \end{bmatrix} \quad (16)$$

$$\Sigma = XC_y'C_yX - XC_y'C_yP - PC_y'C_yX \quad (17)$$

$$P = P' > 0 \quad (18)$$

$$trace(C_2PC_2') < \gamma^2 \quad (19)$$

A. Modification on the existing ILMI algorithm

The ILMI algorithm given by Bervani & Hiyama [5] is modified in three aspects. These are listed below.

(1) The dynamics introduced by the non-ideal implementation of PID controllers are used to define the SOF system.

(2) Constraints are put on the gain margin and phase margin of the loop transfer function. Gain and phase margin of the system are best indicator of system stability in the classical sense. It also avoids premature termination of the algorithm and gives the designer one more design parameter to tune the algorithm to obtain desired performance.

(3) **Problem:** The previous algorithm can get into an infinite loop when the solution for α(j) > 0 and $\alpha(j-1) > 0$. In this case the algorithm will keep minimizing trace(X) to get X come close to P but may never come out of that loop. **Solution:** The solution is to increase the optimum H_2 performance index(γ(j)) for which solution is sought.

The algorithm may have α(j) > 0 and $\alpha(j-1) > 0$ for the initial iterations. This is the case for higher order system where the PID feedback may has less control authority as compared to a full order robust controller. Hence, the mixed sensitivity H_2 performance index for a full order controller may not be close to the performance index achieved by the PID feedback structure.

The QMI in (16) does not guarantee a monotonously decreasing α with an increase in γ. This is due to the positive semi-definite term $B_w\tilde{K}\tilde{K}'B_w'$ which is added to the left hand side of the original inequality, for converting it to QMI form. The QMI formulation is given by Cao et al. [2], and is used in the ILMI algorithm. This will lead to situations when both α(j) > 0 and $\alpha(j-1) > 0$ are true and the algorithm gets into an infinite loop.

B. The algorithm

1. Find out the SOF representation of the system.
2. Augment the SOF output to obtain the generalized plant.
3. Compute the optimal guaranteed H_2 performance index, γ_{opt}, using *hinfmix* function of MATLAB. This serves as the starting point.
4. Initialize γ to γ_{opt} and increment in γ = $d\gamma$.
5. For Q > 0 , obtain the initial X from the riccati equation below.
$$A_iX + XA_i' - XC_y'C_yX + Q = 0 \quad (20)$$
Where, $X = X' > 0$
Initialize j = 1
6. Using X from previous step, solve for P, $\tilde{K}(j)$, $\alpha(j)$ to minimize $\alpha(j)$ and satisfy the matrix inequalities below,
$$\begin{bmatrix} A_iP + PA_i' + B_wB_w' + \Sigma & B_y\tilde{K} + PC_y' \\ (B_y\tilde{K} + PC_y')' & -I \end{bmatrix} < \begin{bmatrix} P & 0 \\ 0 & 0 \end{bmatrix} \quad (21)$$
$$\Sigma = XC_y'C_yX - XC_y'C_yP - PC_y'C_yX \quad (22)$$
$$P = P' > 0 \quad (23)$$
$$trace(C_2PC_2') < \gamma^2 \quad (24)$$
7. If α(j) < 0 then put γ = γ - $d\gamma$
j = j + 1 ; GOTO step 5
8. Else if j = 1 or if n > 0 and n < 10
Solve, for minimizing trace(P), the below LMI using $\alpha(j)$ and $\gamma(j)$ as constants
$$\begin{bmatrix} A_iP + PA_i' + B_wB_w' + \Sigma & B_y\tilde{K} + PC_y' \\ (B_y\tilde{K} + PC_y')' & -I \end{bmatrix} < \begin{bmatrix} \alpha(j)P & 0 \\ 0 & 0 \end{bmatrix} \quad (25)$$
$$\Sigma = XC_y'C_yX - XC_y'C_yP - PC_y'C_yX \quad (26)$$
$$P = P' > 0 \quad (27)$$
$$trace(C_2PC_2') < \gamma^2 \quad (28)$$
   a. If P has feasible solution then
   Put X = P ; n = n + 1; j = j + 1 ; GOTO Step 6

   b. Else Put γ = γ + $d\gamma$; GOTO Step 6
9. Else if j $\neq$ 1 and $\alpha(j-1) > 0$ Put γ = γ + $d\gamma$; j = j +1 ; GOTO Step 6
10. Else if j $\neq$ 1 and $\alpha(j-1) \leq 0$
Form the closed loop system with feedback gain K(j-1)
$A_{cl} = A_i + B_y\tilde{K}(j-1)C_y$
Find γ_∞ using *normhinf* function in MATLAB.
(If the same control is used at different operating point then find the lowest Gain(GM) and Phase(PM) margin for multiple operating points using the same controller)
   a. If $\gamma_\infty < 1$ and GM $>$ GM_0 and PM $>$ PM_0 then GOTO Step 11

b. Else γ = γ + $d\gamma$; j = j + 1; GOTO Step 5

11. Final Gain $\tilde{K}_f$ = $\tilde{K}$(j-1)
    γ_{opt} = γ - $d\gamma$
12. Find K_{PID} = $M^{-1}\tilde{K}_f$
13. END

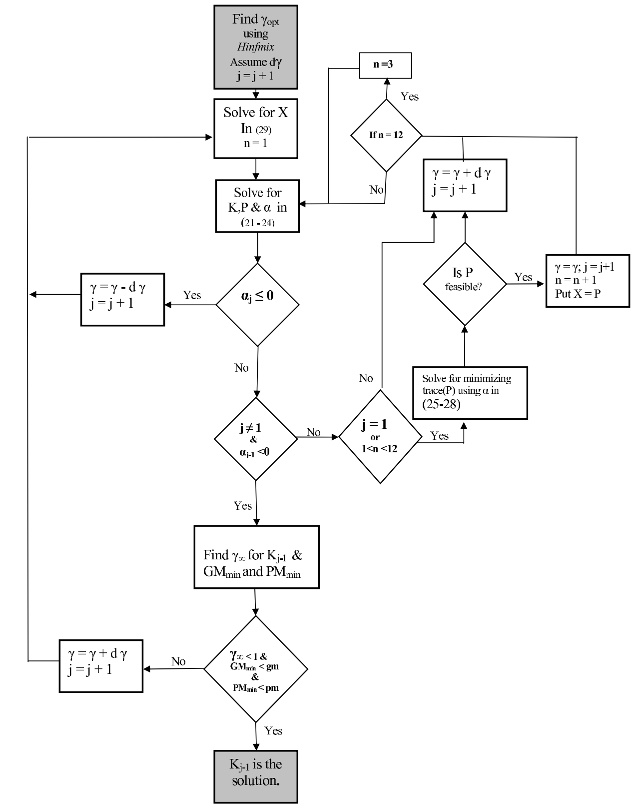

Fig. 3. Flow Chart for Modified-ILMI

IV. Control Design for Micro Air Vehicle

A majority of commercially available low cost hardware that can be put on a micro air vehicle (MAV) permit implementation of simple control logic, such as, P, PI, PD and PID based feedback [8]. These logics use non-ideal implementation of output integrator and differentiator. In order to achieve good performance and stability characteristics, multiple feedback loops of multi-sensor outputs are needed. The feedback has various contradicting requirements like noise rejection, robustness to parameter uncertainty and time domain performance specifications.

The dynamics of Sapthami-flyer, a micro air vehicle, are lowly damped and their natural frequencies of operation are high. This makes it difficult for the pilot to control the aircraft. Unlike conventional aircraft MAV usually employ only aileron control and no rudder control. This is to reduce weight and power consumption. But the dutch roll mode is most effectively controlled by a yaw rate feedback to rudder. The autopilot hardware also has a fixed and limited control structure. Therefore, it is most difficult to get good flying qualities with limited control inputs and limited feedback structures.

A. The system

Sapthami-flyer (see Fig. 4) is an indigenously developed micro air vehicle. It has a span of 31.5 cm which is also its maximum dimension. It carries a camera for a payload and has a requirement for a stable and smooth flight to do ground imaging. More information about the vehicle is given in table I.

TABLE I

Design Parameters of Sapthami-flyer model

Total Weight	191 grams
Wing Profile	Inverse Zimmermann
Wing area	0.074 m^2
Aspect Ratio	1.38
Span	0.315m
Mean Aerodynamic Chord	0.25m
Center of Gravity(X,Y,Z)from nose	(0.077,0,0)m
Aerodynamic Center	0.11m
(I_{xx},I_{yy} ,I_{zz})	(0.00041, 0.0026, -0.00004) kg-m^2
I_{xz}	-0.00004 kg-m^2
Tail area	0.0055m^2
Control Surface Area	0.007 m^2

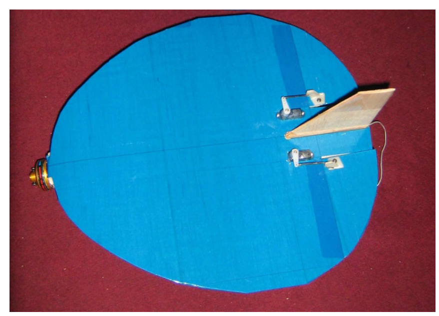

Fig. 4. Sapthami-flyer

B. Control Formulation

A single control is designed to give satisfactory performance throughout the flight envelop. The six degrees of freedom equation of motion for an aircraft are decoupled and linearized into the longitudinal and lateral motion [7]. The equations of motion are linearized for straight and leveled flight at 10 degree angle of attack (α) and are used for control design. Constraints are put while designing to have at least specified gain and phase margins for closed loop linear models at other operating points. The lateral transfer function for sideslip (β), roll angle (ϕ) and yaw rate ($\dot{\psi}$) with respect to commanded aileron (u_{δ_a}) are given below. The dutch roll mode is lowly damped (ξ=0.014) and therefore needs to be improved by feedback.

$$\frac{\beta}{u_{\delta_a}} = \frac{426.294(s^2+2.311s+53.46)}{(s+11.41)(s+0.006091)(s^2+0.2433s+82.06)} \quad (29)$$

$$\frac{\phi}{u_{\delta_a}} = \frac{426.294s(s^2+2.311s+53.46)}{(s+11.41)(s+0.006091)(s^2+0.2433s+82.06)} \quad (30)$$

$$\frac{\dot{\psi}}{u_{\delta_a}} = \frac{-7.2777(s+43.7)(s+11.03)(s-8.684)}{((s+11.41)(s+0.006091)(s^2+0.2433s+82.06)} \quad (31)$$

The controller is implemented on the Kestrel2.22® [9] autopilot hardware which is mounted onboard. The Fig. 5 show the lateral control loop implemented in Kestrel autopilot system. Here, d is the disturbance input of the system and ϕ_d is the desired roll angle. The control helps in performing

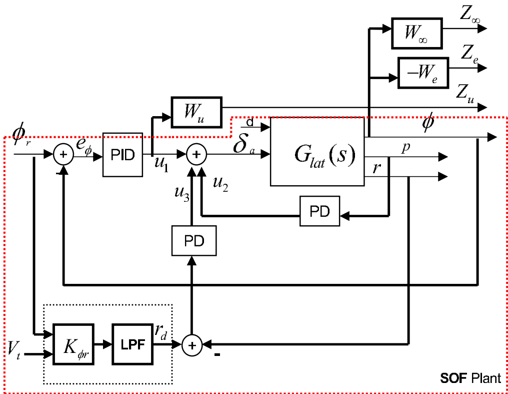

Fig. 5. Lateral Control Loop for Sapthami-flyer

a turn with less sideslip in the absence of rudder control. It tracks the desired roll angle while reducing the side slip. The loop for tracking roll angle uses a PID feedback while the roll rate stabilizing loop uses PD feedback. A desired yaw rate, r$_d$ is commanded as a function of desired roll angle. This is based on the kinematics relation for a coordinated turn given in (32).

$$r_d = \frac{g\cos\theta\ \tan\phi}{V_t} \tag{32}$$

$$K_{\phi r} = \frac{g\cos\theta}{V_t} \tag{33}$$

This desired yaw rate is passed through a low pass filter to avoid high rate of change of desired yaw rate due to measurement noise. The error in yaw rate is fed back through a PD block to the aileron. The performance weights are selected as per guidelines set by the H_2 and H_∞ controller. These are given below and are shown in Fig. 5.

$$W_\infty = \frac{s+1.5}{s+4};\quad W_u = \frac{s+2.2}{s+22};\quad W_e = \frac{100}{s+1} \tag{34}$$

Consider the state space system representation given below.

$$\dot{\mathbf{x}} = A\mathbf{x} + Bu;\ \ \mathbf{y} = [C_1\ C_2\ \ C_3]'\mathbf{x} + Du;\ u = u_1 + u_2 + u_3$$

$$\dot{\mathbf{x_e}} = A_e\mathbf{x_e} + B_e(\phi_d - C_1\mathbf{x});\ \ \mathbf{y_e} = C_e\mathbf{x_e} + D_e(\phi_d - C_1\mathbf{x})$$

$$\dot{\mathbf{x_{d_1}}} = A_{d_1}\mathbf{x_{d_1}} + B_{d_1}C_2\mathbf{x};\ \ \mathbf{y_{d_1}} = C_{d_1}\mathbf{x_{d_1}} + D_{d_1}C_2\mathbf{x}$$

$$\dot{\mathbf{x_{d_2}}} = A_{d_2}\mathbf{x_{d_2}} + B_{d_2}(r_d - C_3\mathbf{x});\ \mathbf{y_{d_2}} = C_{d_2}\mathbf{x_{d_2}} + D_{d_2}(r - C_3\mathbf{x})$$

$$\dot{\mathbf{x}}_{\phi\mathbf{d}} = A_{\phi d}\mathbf{x}_{\phi\mathbf{d}} + B_{\phi d}\phi_d;\ \ r_d = C_{\phi d}\mathbf{x}_{\phi\mathbf{d}} + D_{\phi d}\phi_d$$

Here, the system with states $\mathbf{x}$ represent the plant dynamics without the robust weight augmentation. The non-ideal roll rate and yaw rate PD feedback system dynamics are defined by the states $\mathbf{x_{d_1}}$ and $\mathbf{x_{d_2}}$ respectively. The PID block for roll error feedback has system states $\mathbf{x_e}$. The system with states $\mathbf{x}_{\phi\mathbf{d}}$ gives the desired yaw rate for a desired roll angle. Using the above representations, the SOF formulation for the system in red (see Fig. 5) is found and is given below.

$$\begin{bmatrix} \dot{\mathbf{x}} \\ \dot{\mathbf{x_e}} \\ \dot{\mathbf{x_{d_1}}} \\ \dot{\mathbf{x_{d_2}}} \\ \dot{\mathbf{x}}_{\phi\mathbf{d}} \end{bmatrix} = \begin{bmatrix} A & 0 & 0 & 0 & 0 \\ -B_eC_1 & A_e & 0 & 0 & 0 \\ B_{d_1}C_2 & 0 & A_{d_1} & 0 & 0 \\ -B_{d_2}C_3 & 0 & 0 & A_{d_2} & B_{d_2}C_{\phi d} \\ 0 & 0 & 0 & 0 & A_{\phi d} \end{bmatrix} \begin{bmatrix} \mathbf{x} \\ \mathbf{x_e} \\ \mathbf{x_{d_1}} \\ \mathbf{x_{d_2}} \\ \mathbf{x}_{\phi\mathbf{d}} \end{bmatrix}$$

$$+ \begin{bmatrix} B \\ 0 \\ 0 \\ 0 \\ 0 \end{bmatrix} \tilde{\mathbf{K}} \begin{bmatrix} C & 0 & 0 & 0 & \begin{bmatrix} 0 \\ 0 \\ -C_{\phi d} \end{bmatrix} \\ 0 & I & 0 & 0 & 0 \\ 0 & 0 & I & 0 & 0 \\ 0 & 0 & 0 & I & 0 \end{bmatrix} + \begin{bmatrix} BD_e + BD_{d_2}D_{\phi d} \\ B_e \\ 0 \\ B_{d_2}D_{\phi d} \\ B_{\phi d} \end{bmatrix} \phi_d$$

The open loop SOF system is now augmented with the robust performance weights to obtain the generalized plant function. The augmented system is then used in the algorithm to obtain the PID gains.

V. Results

The feedback tuned gains are given in table II. It must be noted how the derivative gain of roll rate and yaw rate feedback have signs opposite to those of the proportional gains. When the transfer function of I(s) and D(s) are considered then the total feedback transfer function H(s) is found to be stable and minimum phase. If the feedback is designed with the ideal PID implementation, then the actual feedback is very different from that which is designed. The phase margin

TABLE II

Feedback Gains for Sapthami-flyer

Loop	Proportional	Integral	Derivative
Roll Rate	-0.1012	0	0.0014
Yaw rate	-0.0110	0	0.0058
Roll	0.0838	0.0320	0.0004

achieved for the closed loop system is 57.5 degrees. The bode plot of the system is shown in Fig. 6. Design parameters like phase margin and gain margin are crucial. The system is often subjected to control delay. The main reason for the delay being the disturbance in the communication link between the ground station and the autopilot. The autopilot and ground control software itself introduces computation delay upto 0.02ms. In such a situation it is very important to ensure that the feedback control does not make the system unstable. A gain margin ensures system stability in presence of change in loop gain.

A. Simulation study for Loiter Mode

The micro air vehicle under study is flown in various autonomous modes of operation. The loiter mode, is one such mode in which the micro air vehicle circles above the ground with a specific turn radius. In this mode a constant roll angle is commanded by the higher navigation loop. The autopilot employs altitude control also to maintain height. Altitude error commands a pitch angle which in turn commands an elevator deflection. Closed loop nonlinear tracking response to 5 degree roll angle commanded by the navigation loop is

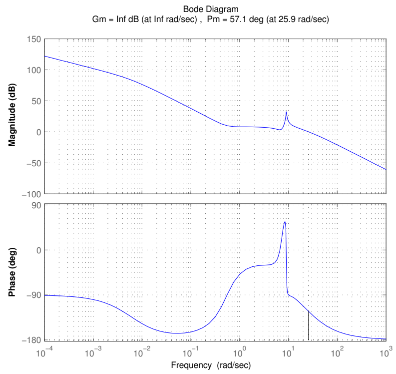

Fig. 6. Bode plot for the loop transfer function

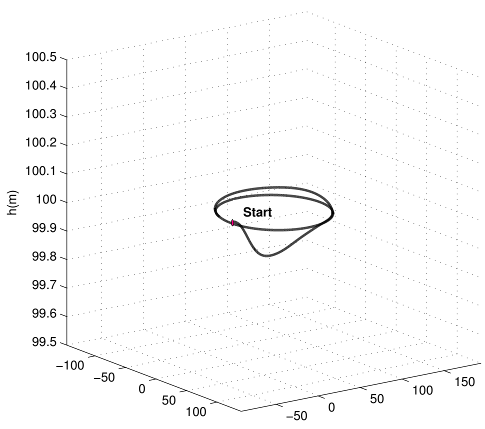

Fig. 7. Loitering with 5 degree roll angle commanded

shown in (Fig. 7 to 9). The settling time for the roll angle is about 20 seconds. The vehicle circles with a non zero sideslip (Fig. 8). The sideslip has amplitude less than 0.5 degrees. This is due to the aileron having less authority on the directional motion. The mission performed by the vehicle do not have requirement for perfect coordinated turn, hence the response is satisfactory.

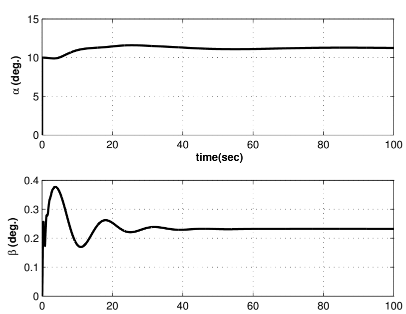

Fig. 8. Angle of attack (α) and Sideslip (β)

VI. Conclusion

The iterative matrix inequality algorithm has been improved and extended for the systems having non-ideal PID implementations. The integrator and differentiator implementations effect the feedback and reduces its authority. The design presented takes into account constraints to come up with an acceptable controller that can be implemented on a practical hardware onboard an MAV.

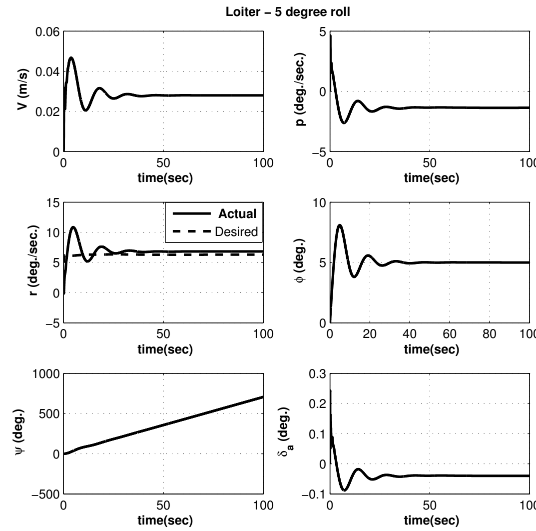

Fig. 9. Lateral states and control

References

[1] Shinn-Jang Ho, Shinn-Ying Ho, Ming-Hao Hung, Li-Sun Shu, and Hui-Ling Huang (2005). Designing Structure-Specified Mixed H_2/H_∞ Optimal Controllers Using An Intelligent Genetic Algorithm Iga, *IEEE Transactions On Control Systems Technology, Vol. 13, No. 6*, November 2005

[2] Yong-Yan Cao, James Lam and You-Xiam Sun(1998). Static output feedback stabilization: An ILMI apporach *Automatica Vol. 34, No. 12 pp 1641-1645, 1998.*

[3] P.Cominos and N.Munro(2002). Pid Controllers: Recent Tuning Methods And Design To Specification ,*IEE Proceedings online no. 20020103*, pp.46-53, Jan 2002

[4] Feng Zheng, Qing-Guo Wang and Tong Heng Lee(2002). On the design of multivariable PID controllers via LMI approach *Automatica 38(2002)517-526*, 2002.

[5] Hassan Bevrani and Takashi Hiyama (2007). Multiobjective PI/PID Control Design Using an Iterative Linear Matrix Inequalities Algorithm *International Journal of Control, Automation, and Systems, vol. 5, no. 2, pp. 117-127*, April 2007.

[6] Mahmoud Chilali and Pascal Gahinet(1996). H_∞Design with Pole Placement Constraints :An LMI Approach *IEEE Transactions On Automatic Control, Vol. 41, No. 3*, pp.358-367, March 1996

[7] J. H. Blakelock, Automatic Control of Aircraft and Missiles, *John Wiley & Sons Publications*, 2nd Edition, 1965

[8] Kestrel User Guide for firmware version MA8.1 & Virtual Cockpit 2.3, Document Version 1.51 *Procerus Technologies*, 2007

[9] Kestrel Autopilot^{TM} , Procerus Technologies. *http://www.procerusuav.com/*

[10] M Meenakshi and M Seetharama Bhat(2006). Robust fixed-order H_2 controller for micro air vehicle-design and validation *Optimal Control Applications and Methods 27(4):pp. 183-210.*, 2006.